GMR
The Original

FENGYCIN/ MIR-34A-FENGYCIN COMPLEX: AN ALTERNATIVE THERAPEUTIC STRATEGY FOR HCT116 COLORECTAL CANCER CELL LINE

Yaser Jasem Alkhatony[1*], Mahmood Abdujabar Altobje[2], and Mahmood Ahmad Aboo [3]

1. Bacteriology Specialist, Al-Baaj General Hospital, Nineveh Health Directorate, Ministry of Health, Al-Zohour Street, Mosul 41002, Iraq. ORCID: 0000-0001-5561-5406
2. Department of Biology, College of Science, University of Mosul, Al-Majmoaa Street, Mosul 41002, Iraq. ORCID: 0009-0007-1402-0749
3. Al-Baaj General Hospital, Nineveh Health Directorate, Ministry of Health, Al-Arabee Street, Mosul 41002.
*Corresponding Author: Yaser Jasem Alkhatony.
Email: Yaser.23scp153@student.uomosul.edu.iq

Abstract

Background. The development of selective anticancer therapies remains a major challenge due to tumor heterogeneity and limited specificity of conventional treatments.
Aim: This study designd to evaluate the cytotoxic effect of fengycin/fengycin-miR-34a complex toward growth and proliferation of HCT116 colorectal cancer cell line.
Materials and methods: The interested protein in current study was extracted previously by the supplying company, MTT assay was used to evaluate the effects of fengycin/miR-34a-fengycin complex on cancerous HCT116 and Homo sapiens gingival fibroblast (HGF) cell line at variant dilutions (20, 30, and 40 µg /ml), RT-qPCR was depended to detect focused gene expression of K-ras, PIK3CA, TP53, and caspase-3 genes in both cell lines.
Results: Fengycin exhibited a dose-dependent increase in apoptosis in HCT116 colorectal cancer cells (5%, 27.6%, and 60% at 20, 30, and 40 µg/mL, respectively), with minimal effects on normal HGF cells (3%, 1%, and 4%; P=0.001). Transfection with miR-34a alone reduced HCT116 cell viability to 39.7%, while maintaining high viability in HGF cells (117%). Notably, the miR-34a–fengycin biocomplex (30 µg/mL protein / 2.5 nM miRNA) demonstrated the highest apoptotic rate in HCT116 cells (71.6%) compared to only 9.6% in HGF cells (P= 0.01). At the molecular level, this treatment significantly upregulated TP53 and caspase-3 expression (36.7- and 47.5-fold, respectively), with minimal changes in KRAS (1.1-fold) and slight elevation in PIK3CA (1.7-fold). In contrast, HGF cells showed marked upregulation of survival-related PIK3CA (442.9-fold) and KRAS (28.6-fold), with limited apoptotic signaling.
Conclusion: The miR-34a–fengycin biocomplex exerts potent and selective anticancer activity by enhancing apoptosis in cancer cells while preserving normal cell viability. This dual-action strategy highlights its potential as a promising targeted therapeutic approach for colorectal cancer.

Keywords: Colorectal cancer, fengycin, miRNAs, miR-34a, HCT116 cell line, cell line transfection.

1. INTRODUCTION

Colorectal cancer is the third most common cancer globally, with over 1.9 million new cases diagnosed in 2022, and it is the second leading cause of cancer related deaths, resulting in more than 900,000 deaths annually. Early diagnosis programmers can reduce delays in receiving care after symptom onset. Treatments are more likely to cure the disease in the early stages. In settings with organized screening programmers, regular screening is the most effective way to detect colorectal cancer early and prevent the disease through the identification and removal of precancerous lesions. Screening has been shown to reduce both incidence and mortality [1].
The pathogenesis of colorectal cancer primarily stems from the gradual accumulation of genetic mutations, which drive oncogene (KRAS) activation and tumor suppressor gene (TP53) inactivation [2,3].

Bacillus species produce fengycin, a rhizosphere-derived lipopeptide with strong antibacterial and anticancer effects [4]. The first and most important stage in fengycin biological effects is its insertion into the lipid bilayers of cellular membranes; this interaction with the membrane is concentration-dependent and results in notable changes to the structure and function of the membrane [5].
The anticancer mechanism of fengycin is mainly attributed to the induction of apoptosis in cancer cells. This process is initiated by the generation of intracellular reactive oxygen species (ROS), which leads to mitochondrial dysfunction. The damaged mitochondria release pro-apoptotic factors like cytochrome c into the cytoplasm. Fengycin has demonstrated significant cytotoxic effects against various human cancer cell lines, suggesting its potential as an anticancer agent. Caspases (like caspase-3 and -9) are activated and apoptosis is carried out as a result of a series of events that include the overexpression of the pro-apoptotic protein Bax and the downregulation of the anti-apoptotic protein Bcl-2 [6].
Micro-RNA (miRNA)-mediated gene silencing has advanced significantly since its discovery in 1998. This highly conserved method of post-transcriptional gene silencing is mediated by miRNA molecules [7].
Regarding the function of miRNAs in lung cancer, miR-34a has been shown to function as a tumor suppressor by targeting many genes linked to cell proliferation and death. It maps to a region of chromosome 1p36 that is frequently deleted [8].
Unlike previous studies investigating miRNAs or fengycin separately, the current study explores a combined MiR-34a–fengycin biocomplex as a selective anticancer strategy targeting apoptotic pathways in HCT116 colorectal cancer cells. In addition, the study highlights the potential synergistic interaction between MiR-34a-mediated gene regulation and fengycin-associated cytotoxic activity

2. MATERIAL AND METHODS

2.1. Preparation of Experimental Reagents and Transfection Complexes

2.1.1. Preparation of fengycin protein concentrations

Fengycin protein was obtained from Lipofabrik (Elephant Vert Group, France) and dissolved in dimethyl sulfoxide (DMSO) (Sigma-Aldrich, Germany). Briefly, 200, 300, and 400 µg of fengycin were dissolved in 1 mL of DMSO to obtain intermediate concentrations of 200, 300, and 400 µg/mL, respectively.
A volume of 95 µL of cell suspension at a density of 1×10^4 cells/well was seeded into each well of a 96-well microplate and incubated for 24 h under standard culture conditions to allow the formation of a confluent monolayer
For protein treatment, the final working concentrations were prepared directly in the wells by adding 5 µL of each original stock solution to 95 µL of the pre-seeded cell suspension, resulting in a total final volume of 100 µL per well. Based on the dilution equation ($C_1V_1 = C_2V_2$), the initial stock concentrations of 400, 600, and 800 µg/mL yielded final concentrations of 20, 30, and 40 µg/mL, respectively.

2.1.2. Preparation of miRNAs solution

MicroRNA molecules were reconstituted by adding 300 µL of nuclease-free deionized water to obtain a stock solution with a final concentration of 100 nM. Subsequently, the transfection mixture was prepared by combining 250 µL of Lipofectamine 3000 with 250 µL of miR-34a solution at 100 nM, resulting in a final concentration of 2.5 nM in the transfection mixture.
For cellular transfection, 5 µL of the prepared transfection mixture was added to each well of a 96-well plate containing 95 µL of cell suspension, giving a total final volume of 100 µL per well. Accordingly, the final concentration of each miRNA within the well was 2.5 nM.

2.1.3. Preparation of miRNA–Fengycin Transfection Complexes

The transfection complexes were prepared by mixing 500 µL of RNAifectin solution containing miR-34a at a concentration of 2.5 nM with 500 µL of each Fengycin protein concentration (400, 600, and 800 µg/mL). After mixing at a 1:1 (v/v) ratio, the final volume of each formulation was 1 ml.
Accordingly, the final concentrations of Fengycin protein in the prepared complexes were 200, 300, and 400 µg/mL, respectively, while the final concentration of miRNA was reduced to 25 nM. These formulations were subsequently used for cellular transfection experiments.
The final concentrations of the miRNA–Fengycin transfection complexes after adding 10 µL to 90 µL of cell suspension were 2.5 nM for miRNA and 20, 30, and 40 µg/mL for Fengycin protein, respectively.

2.2. Cell lines preparation and culture

Homo sapiens-HCT116 (CCL-247 ™, passage 10), and homo sapiens gingival fibroblast, HGF-1(CRL-2014 passage. 15) cells were supplied by ATCC®, they were activated in to DMEM high glucose (basal medium, 10% fetal calf serum, FBS, and 0.5% penicillin/ streptomycin antibiotics) and incubated at 37C at 5% CO_2 for overnight, after that they were seed at the same gradient of DMEM except 6% of FBS then they examined until forming monolayer (confluence between 70-80%).

Three milliliters of trypsin were then added to the cell line flask and incubated until the cells detached, then medium was discarded, cells were washed with 1X PBS to get rid of any leftover media, two milliliters of DMEM were added to inactivate the trypsin and the cells were precipitate at 2500 rpm\min, noticed cells pellet was collected by suspend them with one of medium, for investigation cellular activity 10 µl of trypan blue (sigma-Aldrich, Germany), was mixed with 10 mm of cellular suspension, the mixture was distributed between cover slide and Neubauer's chamber to demonstrate the living cells and counting them [9].

2.3 Cell counting

After loading 10 µl of staining cell mixture onto hemocytometer's grid-lined section, four of 16 squares were counted. The average was calculated. The cell number in 1 ml was calculated via multiplying the final average by $10^{4.}$ the volume was stuffed to 9 ml with growth media, final concentration of the cells in the medium was 10^6\10 ml, so 10^4\100µl was the final concentration of the cell foe each well. Similarly, same steps experiment was conducted with HGF cells, seeding cells into 96-well plate [10].

2.4. MiR-34a/ miR-34a-fenfycin transfection

2.4.1 Seeding cells treating

According to Freddy et al. (2015), confluence of the cells was exposed to present protein (20, 30, and 40 µg/ml) to detect fengycin bioactivity. Ninety five microliters of the medium with seeded cells (10^4 cell/well) were contained in each well of 96-well plate, and 5 µl of fengycin protein concentration (20, 30, and 40 µg/ml) were added with three replicates wells for each concentration, three replicates wells for mixture DMSO, medium and seeding cells (protein solvent), three replicates wells for miR-34a (2.5Nm/100 µl) , three wells for each of miR-34a-p1, miR-34a-p2, and miR-34a-p3, and three replicates wells had medium with seeding cells, final volume for each interested well was 100 µl.

2.4.2 Fengycin exposure and of biological complex transfection

According to Freddy et al., (2015), Cells were seeded in 96-well plates at a density of 1×10^4 cells/well in 90 µL medium. Then, 10 µL of fengycin (20, 30, and 40 µg/mL) was added. Experimental groups included fengycin alone, miR-34a alone, MiR-34a–fengycin biocomplex, DMSO control, and untreated control. Each group was performed in three replicates with a final volume of 100 µL per well. Plates were incubated for 24 hours at 37°C with 5% CO_2. The same protocol was applied to HGF cells.

For MiR-34a transfection, 5 µL of the RNAifectin–MiR-34a transfection mixture containing MiR-34a at a final concentration of 50 nM was added to each culture well containing 95 µL of complete culture medium. The transfection process was performed under sterile conditions according to the manufacturer's instructions to ensure efficient intracellular delivery of the miRNA. Each treatment was conducted in three independent replicates to ensure reproducibility and statistical reliability of the experimental results.

For MiR-34a-fengycin biocomplexes, a volume of 10 µL from each prepared transfection biocomplex was added to the cultured cell wells containing 90 µL of complete culture medium. All treatments were performed under sterile conditions.

Blank wells were prepared by adding 10 µL of DMSO suspension to cultured cell wells containing 90 µL of complete culture medium, as described previously.

Control wells were prepared by seeding viable cells (1×10^4 cells/100 µL) in 100 µL of DMEM culture medium without any biological treatment. three independent replicates were included to monitor normal cell growth, maintain experimental baseline conditions, and exclude potential contamination during the incubation period.

2.4 Validation assays

2.4.1. Cell proliferation evaluates

The MTT kit (Biotium,USA)was used for determining living cell numbers by absorbance using micro plate reader to conduct cell viability (according to manufacturer protocol), working solution was prepared immediately and incubated at 37°C, Briefly, added to each targeted well need to be test.

After incubation,10µl of MTT solution (3-(4,5 dimethyl-2-thiazolyl)-2,5-diphenyl tetrazolium bromide) was added to each targeted well, then 96wells was incubated for 4 hours at 37ºC and 5% CO_2, after that 200µl of DMSO was added to each well. Finally, the absorbance was measured with ELISA Reader (Thermo, china) at wave length of 630 nm. During the current investigation, cell viability was determined using the following mathematical formula: Cell viability = (OD of treated cell-OD of blank) x100\ (OD of control-OD of blank) [11,12].

2.4.2 Transfection efficacy

2.4.2.1. MicroRNA extraction and complementary DNA synthesis

MicroRNA was isolated according manufacturer instructions of supplied company(Geneaid, Taiwan).Specific Primers were used for Reverse Transcription(3-GTCGTATCCAGTGC AGGGT CCGA GG TATTCGCACTGGATACGACTTTTTTTTTTTVN-5,Mcrogen, south Korea)and snRNA-RNU6 was (3-G CTTCGGCAGCACATATACTAAAATB-5.Ella Biotech,Germany)The master mix was supplied by Wizbio (South Korea).Amplification mixture was included (2µl)RTase Reaction Buffer(10X),(1µl)primer (10nM),(1µl)dNTP mix(20X),reverse transcriptase(1µl),RNase Inhibitor(1µl)and RNase free(9µl),miRNA template(3µl) and 2µl of M-DTT(0.1), final reaction volume was 20µl.Amplification conditions were included two steps, 50°C for 60min, and 10°C for 1min.

2.4.2.2. Detection of original and mimic transfected miR-34a copy number in targeted cells

Complementary strand of DNA was frizzed at -20ºC. The specific primer set was used for detection transfection efficacy were designed in this study, they include miR-34a-F(3-GTCGTATCCAGTGCAGGGT -5), R(3- AACAAGTGGCAGTGTCTTAGC -5, Macrogen, south Korea) andsnRNA-RNU6-F(3-GCTTCGGCAGCACATATACTAAAAT-5),R(3-CGCTTCACGAATTTGCGTGTCAT-5,).Mixture of quantitative hybridization was prepared with final volume 20µl(2X SYBR-Green Master Mix(10µl), Forward Primer10 µM , (1µl), Reverse Primer 10 µM(1µl),cDNA template (5µl),RNase free,3µl, all amplification solution were provided by Wezbio /South Korea).Then the 200µl tubes were subjected to Rotorgen thermocycler (QIAGEN,Germany). Conditions for Real quantitative amplification involve 40cycles Denaturation, 95C(6min), primer hybrid-dization,60(45second).

2.4.3. Estimation of interested Gene transcription

This study evaluated four genes to determine the way fengycin affected the expression of the tumor suppressor gene TP53, the oncogene K-ras, the late stage of apoptotic genes (Caspase-3), and the PIK3CA gene, which is regarded as one of the most significant markers of cellular activity and a transcription factor that activates the activity of numerous molecular pathways in living cells.

2.4.3.1 Interested functional complementary DNA strands synthesis

Messenger RNA isolation was conducted according to instruction of manufacturer company (Geneaid, Taiwan). Specific Primers were used for Reverse Transcription (GTCGTATCCAGTGCAGGGTCCGAG G TATTCGCACTGGATACGACTTTTTTTTTTTVN, Macrogen, south Korea) and snRNA-RNU6 was (3p-G CTTCGGCAGCACATATACTAAAAT, Ella Biotech, Germany). The master mix was supplied by Wizbio (S.Korea).Amplification mixture was included 10X RTase Reaction Buffer(2µl),primer(1µl),20X dNTP mix(1µl),reverse transcriptase(1µl), RNase Inhibitor(1µl) and RNase free(9µl),miRNA template(3µl) and (2µl)of 0.1 M-DTT to complete the final volume as 20µl.Amplification conditions were included two steps, 50°C for 60min, and 10°C for 1min. as cooling temp.

2.4.3.2 Interested functional genes expression

Target primers were utilized to detect expression of specific molecular markers were designed in study include,β-Actin(Referencegene)-F-(3-CATGTACGTTGCTATCCAGGC-5),R-(3-CTCCTTAATGTCACGCACGAT-5);K-ras(oncogene)-F-(3-TCGACACAGCAGGTCAAGG-5),R-(3-

CAAAGAAAGCCTCGT -5);TP53(Tumor suppressor)-F-(3-CAGCACATGACGGAGGTTGT-5),R-(3-TCATCCAAATAC TCC A CACGC-5);PI3KCA(cell proliferation transcription factor)-F-(3-TAATGCTTGGGAGGATGCCC-5), R-(3-GGTGTAGCTGTGGAAATGCG-5)and Caspase-3(apoptotic late stage)-F-(3-CCTAGCGGATGG GTGCTATT-5),R-(3-CGGATACAC AGCCACAGGTA-5).The present primers were provided by Macro gen company(South Korea),except β-Actin was provided by Ella-biotech company (Germany).
Amplification mixture included 3µl of mRNA Template,1µl of hexamer -primer,1µl of dNTPs,1µl of RNase-Free Distilled Water, 9µl(10X)of RTase Reaction Buffer,2 µl(0.1)of M-DTT,2µl of Reverse Transcriptase, 1µl RNase to complete the final volume as 20µl. Hybridization conditions involve 40cycles for each of Denaturation,95C(6min) and primers annealing were β-Actin(60ºC), K-ras(60ºC), TP53(57.5 ºC), PI3KCA (60ºC), Caspase-3(61ºC), whereas primer hypridization time was 45second for all of them.

2.5. Biostatical analysis
All experiments were performed in triplicate, and the data are expressed as mean ± standard deviation (SD). Statistical analyses were conducted using GraphPad Prism version 9.0 (GraphPad Software, San Diego, CA, USA). Differences among experimental groups were analyzed using one-way analysis of variance (ANOVA) followed by Tukey's post hoc test. A p-value < 0.05 was considered statistically significant.
"To evaluate the differential response between HCT116 and HGF cell lines, an Independent Samples t-test was conducted for each experimental parameter (cell viability, transfection efficiency, and relative gene activities). Data are expressed as relative fold changes. Statistical significance was defined as $P < 0.05$.
Relative transfection efficiency and miR-34a expression levels in HCT116 and HGF cells used an unpaired t-test comparing each treatment group with the control group, Statistical significance was defined as $P < 0.05$.
Microsoft Excel software (Microsoft Corp., USA) was used for data processing and calculation of cell viability percentages. In addition, gene expression levels were analyzed using the comparative threshold cycle (ΔΔCt) method, as described by Livak and Schmittgen [13].
Briefly, the relative expression levels were calculated as follows:
ΔCt = Ct (target gene) − Ct (reference gene), $\Delta\Delta Ct = \Delta Ct(\text{treated}) - \Delta Ct(\text{control})$,
Fold change = 2^−ΔΔCt,

Ethical committee approval
"The present study was conducted on established human cancer cell lines (HCT116) and did not involve human participants or experimental animals. Therefore, formal ethical committee approval was not required according to institutional guidelines. Date and number of protocols: Not applicable."

3. RESULT

2.6.1. Biological effect of fengycin protein on HCT116 and HGF cell proliferation
MTT test was used to assess the biological effects of fengycin on both HCT116 and normal HGF cell lines. The results of the current study showed the Fengycin treatment dramatically and dose-dependently increased apoptosis rate in the HCT116 colorectal cancer cell line (5, 27.6, and 40%) at concentrations (20, 30, and 40µg /ml), respectively, compared with apoptosis of HGF cell line (3, 1, and 4%), respectively, (P=0.001), (**Table 1**).
The second and third concentrations of fengycin (30, and 40µg/ml) had highest therapeutic index which had apoptotic value 27.6% and 40%, respectively, in comprehensive with their apoptotic value in HGF cells 1% and 4%, respectively, (P=0.001), while the first concentration of fengycin (20µg/ml) had lowest therapeutic index that had apoptotic value 5%, compared with 3% in HGF cells, (P=0.856).

Table 1: Effect of Fengycin concentrations on cell viability and apoptosis of both cell lines.

Treatment / Group	OD 1	OD 2	OD 3	Mean OD ± SD	HCT116 Viability (%)	HCT116 Cytotoxicity (%)	HGF Viability (%)	HGF Apoptosis (%)
Blank	0.220	0.185	0.221	0.208 ± 0.004	-	-	-	-

control	0.643	0.614	0.618	0.625 ± 0.016	100.0	0.0	100.0	0.0
20 **µg/mL**	0.607	0.607	0.598	0.604 ± 0.005	95.0	5.0	97.0	3.0
30 **µg/mL**	0.515	0.508	0.507	0.510 ± 0.004	72.4**	27.6**	99.0	1.0
40 **µg/mL**	0.460	0.458	0.456	0.458 ± 0.002	60.0***	40.0***	96.0	4.0

OD, Optical Density; SD, Standard Deviation; DMSO, Dimethyl sulfoxide; HCT116, Human colorectal carcinoma cell line; HGF, Human gingival fibroblasts. $p < 0.01$ and * $p < 0.001$\$ indicate highly significant differences when compared to the untreated control group using Tukey's HSD post-hoc test.

The protein-treated cells' microscopic appearance underwent several alterations, such as the nuclei in those cells disappeared, it was noted that the shape of apoptotic cells changed from spindle or cuboidal to spherical, with the presence of black dots signifying changes in the internal content of the cells. In the meanwhile, the cell viability rates were consistent with the density of cells with changed shapes and the existence of clusters of dead cells or cells going through cell death as bright or dark foci (**Figure 1**).

Figure 1: Morphological Changes and Apoptotic Features in Treated Cells Observed by Phase-Contrast Microscopy. A: control A549 cells, B: A549 cells after treating with 40 µg/mL fengycin.

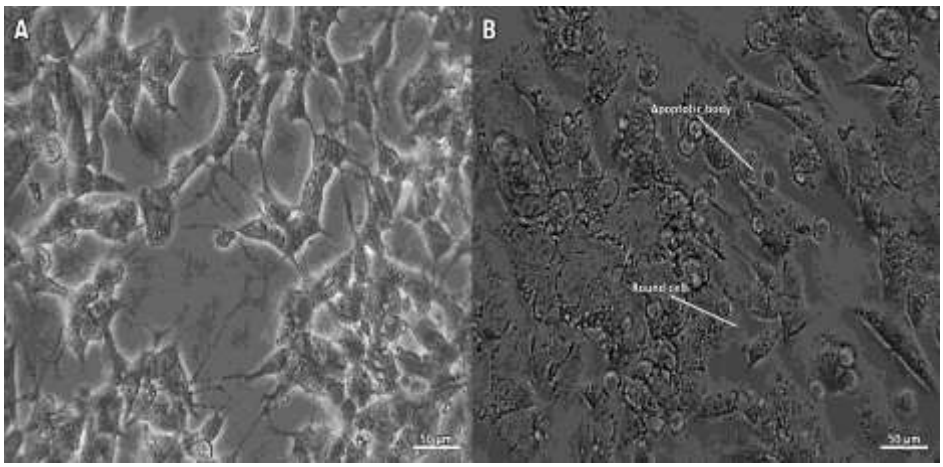

At molecular level, the effect of various treatment doses on certain genes in both HCT116 and HGF cell lines were assessed using gene expression analysis. K-ras, TP53, PIK3CA, and caspase-3 genes were among the genes examined. A change of 1 was used to equalize the control group.
After treatment of HCT116 cells with 30 and 40 µg/mL of the protein induced a marked activation of apoptotic signaling pathways. This effect was evidenced by the significant upregulation of Caspase-3, with expression levels increasing to 1.01- and 1.78-fold at the second and third concentrations, respectively. Concurrently, a pronounced downregulation of the oncogene K-ras was observed, with expression reduced to 0.7- and 0.41-fold, respectively, indicating suppression of proliferative signaling, (**Figure 2**).

Figure 2: Gene activity of interested genes in HCT116 cells

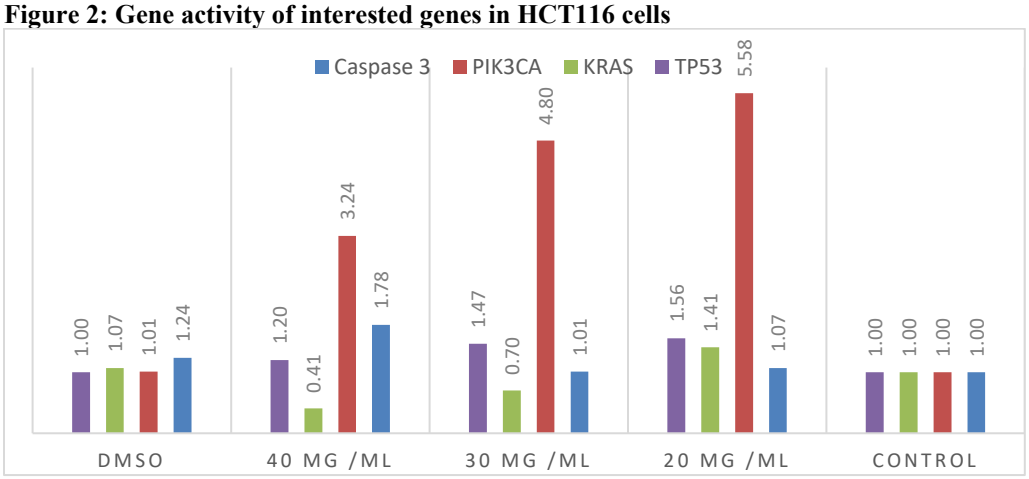

Furthermore, the expression patterns of TP53 and PIK3CA suggest a concentration-dependent interplay between pro-apoptotic and survival pathways. Specifically, TP53 gene expression showed modulation with values of 1.47- and 1.20-fold, while PIK3CA gene expression exhibited strong changes at 4.8- and 3.24-fold for the second and third concentrations, respectively. Collectively, these findings indicate that the treatment not only promotes apoptosis but also differentially regulates key genes involved in cell survival and tumor progression in a dose-dependent manner. Additionally, The DMSO group showed no significant deviation from control (1.24-fold), (figure 2).

On the other hand, after treatment of normal HGF cell line, the PIK3CA gene reported a high level of gene expression at 30, and 40 µg /ml, (1.91, and 2.2-fold), respectively, while, the oncogene K-ras, tumor suppressor TP53, and caspase-3 gene activity was very close to the control value, (figure 3).

Figure 3: Gene activity of interested genes in HGF cells

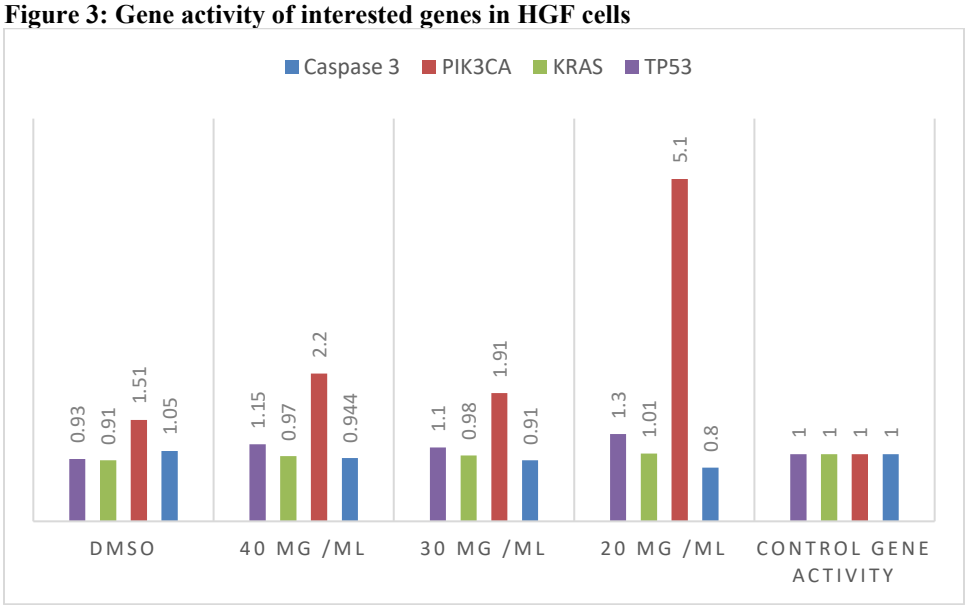

2.6.2. Biological effect of fengycin/miR-34a-fengycin complex on cell lines

The results of the present study demonstrate a significant biological effect of miR-34a on the HCT116 colorectal cancer cell line. This effect was characterized by a marked reduction in cell viability, reaching 39.7% ($P < 0.01$), indicating a strong cytotoxic or growth-inhibitory response. Morphological examination

further supported these findings, revealing the formation of clustered, dark-stained cells with a predominantly spherical shape following transfection, suggesting the induction of cellular stress and potential apoptotic processes, (Table 2).
In contrast, the normal HGF cells exhibited no significant reduction in viability, maintaining a relatively high survival rate 117%. These observations highlight the selective anticancer activity of miR-34a, suggesting its potential role as a therapeutic regulator capable of targeting malignant cells while sparing normal cells.

Table 2: cell viability and apoptotic value of miR-34a-fengycin complex.

Treatment Group	Cell line	OD1	OD2	OD3	Mean ± SD	Viability (apoptosis) %	Tukey P-value (vs Control)
miR-34a	HCT116	0.58	0.531	0.544	0.552 ± 0.025	39.7(60.3)	p < 0.001 ***
	HGF	1.178	1.117	1.134	1.143 ± 0.031	117(0)	p < 0.001 ***
miR-34a-p1	HCT116	0.766	0.717	0.73	0.738 ± 0.025	64(36)	p < 0.001 ***
	HGF	0.811	0.762	0.777	0.783 ± 0.025	70(30)	p < 0.001 ***
miR-34a-p2	HCT116	0.493	0.444	0.459	0.465 ± 0.025	28.4(71.6)	p < 0.001 ***
	HGF	0.962	0.923	0.934	0.940 ± 0.020	90.4(9.6)	p < 0.05 *
miR-34a-p3	HCT116	0.671	0.622	0.635	0.643 ± 0.025	51.6(48.4)	p < 0.001 ***
	HGF	0.867	0.818	0.833	0.839 ± 0.025	77.3(23.7)	p < 0.001 ***
Control		1.016	1.022	1.001	1.013 ± 0.011	100	Reference
Blank		0.328	0.198	0.218	0.248±0.012	0	—

OD: optical density, P1, P2, and P3: fengycin concentration at 20, 30, and 40 µg \ml respectively.

However, the results of our investigation showed that the biological efficacy of miR-34a and transfection complexes (miR-34a-fengycin) against both cancer HCT116 and normal HGF cell lines varied. MiR-34a-P2 (30 µg\ml of protein /2.5nMl of miRNA) had the highest therapeutic index (48.4%) when transfected in the HCT116 cell line, although miR-34a-p3 (40 µg\ml of protein /2.5nM of miRNA) had the highest concentrated protein (40 µg\ml), but had low therapeutic index because of increasing of apoptotic value of miR-34a-p3 (23.7%) toward HGF cells compared with (9.6%) for miR-34a-p3.
Similarly, treatment with the transfection complex miR-34a-p1 (20 µg\ml of protein /2.5nML of miRNA) resulted in a pronounced cytotoxic effect, with an apoptotic value of 36% observed in HCT116 cancer cells. However, despite this apparent efficacy, its therapeutic index is limited due to a lack of selectivity, as it also induced a markedly elevated level of cytotoxicity in normal cells, reaching 30%. This substantial increase in cell death among healthy cells indicates nonspecific toxicity, thereby reducing its suitability as a safe therapeutic candidate. (Table 2).

Figure 4: morphology of HCT116 cell line, A; untreated HCT116 cell line B; HCT116 treated with miR-34a alone, C-E; cell lines after treatment with miR-34a-p1. MiR-34a-p2, and miR-34a-p3, respectively, 40 X on the inverted microscope.

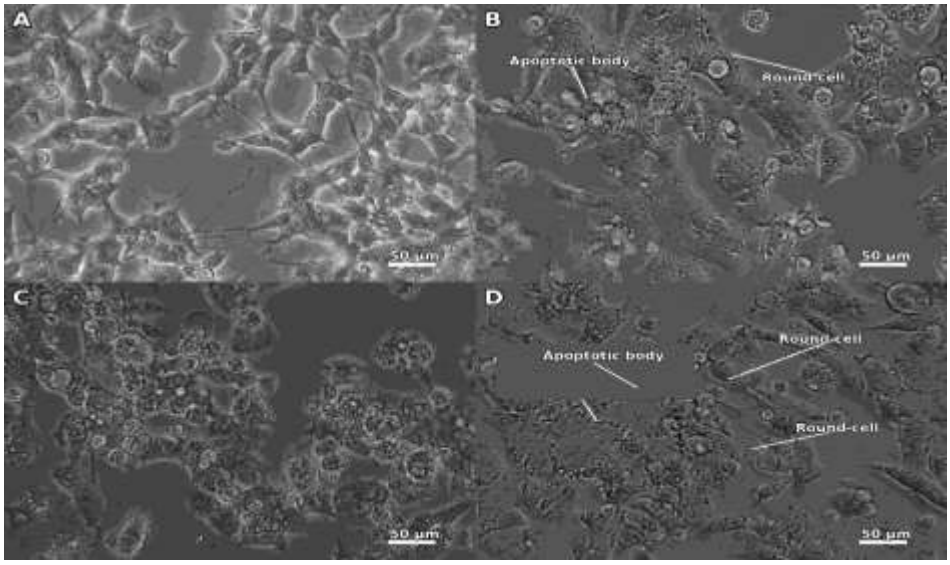

At molecular level, the transfection complex's gene expression was only assessed at 30 µg\ml protein/ 2.5 nM miRNA (miR-34a-p2), due to its high therapeutic index; the other transfection complexes were not included due to their low therapeutic index (low selective toxicity).
After transfection of mRNA-fengycin in both cell lines, significant changes in gene activity were noted. Strong activation of the apoptotic pathway was shown by the 36.7, and 47.5-fold increase in tumor suppressor TP53 and caspase-3 in HCT116 cells, respectively. A slight 1.7-fold increase in PIK3CA activity was seen. K-ras activity, on the other hand, was very closed to baseline (1.1-fold), at a significance level P-value <0.001, (Table 3).

Table 3: relationship between apoptotic rate and gene activity of interested genes of miR-34a-p2 complex.

Cell lines	Cell viability (apoptosis) %	Transfection efficiency	K-ras Relative Activity	TP53 Relative Activity	Caspase-3 Relative Activity	PIK3CA Relative Activity
HCT116	28.4 (71.6)	52.3	1.1	36.7	47.5	1.7
HGF	90.4 (9.6)	58.1	28.6	7.5	1.7	442.9
T-value	21.401	11.235	5.241	6.115	8.354	31.45
P-value	< 0.001	< 0.001	0.006	0.003	< 0.001	< 0.001

On the other hand, after transfection of miR-34a-p2 in HGF cells, K-ras gene activity significantly enhanced (28.6-fold). While caspase-3 activity only modestly increased (1.7-fold), tumor suppressor TP53 gene activity rose considerably (7.5-fold). Strong activation of cell survival signaling pathways was indicated by the notable 442.9-fold increase in PIK3CA activity at a significance level P=0.001, (Table 3).
In addition, the two cell lines had different transfection efficiencies. HGF cells demonstrated a greater transfection effectiveness of 58.1-fold in comparison to the control group, whereas HCT116 cells showed a 52.3-fold increase. HGF cells maintained high viability despite their increased transfection efficiency, suggesting that transfection was not the only cause of the apoptosis seen in HCT116 cells, (Table 3).
Also, after transfection, cell viability showed a significant difference between the HCT116 and HGF cell lines. The percentage of apoptotic cells in the HCT116 cells increased to 71.6%, indicating a significant induction of programmed cell death, while viability was decreased to 28.4%. HGF cells, on the other hand, demonstrated 90.4% viability with just 9.6% apoptosis, indicating that the therapy had little deleterious impact on normal fibroblast cells, (Table 3).

4. DISCUSSION

Cancer is a complex and intractable disease due to genetic and epigenetic heterogeneity, including mutations and telomeric alterations, this heterogeneity significantly affects treatment response and therapeutic outcomes [14,15].

The present study showed that fengycin selectively inhibits cancer cell proliferation while having minimal effects on normal HGF cells. This selectivity may result from differences in genetic background, membrane composition, and signaling pathways between normal and malignant cells. In addition, fengycin activity is dose-dependent, which plays a critical role in determining its anticancer efficacy [16,17].

Fengycin's mechanism of action is primarily related to membrane disruption. It forms pores in lipid bilayers, leading to leakage of intracellular components and cell death. At low concentrations, it induces pore formation gradually, while at high concentrations it acts like a detergent, causing rapid membrane solubilization [18].

The present study further demonstrated that fengycin induces selective cytotoxicity in HCT116 colorectal cancer cells, consistent with previous reports, fengycin derived from Bacillus subtilis inhibited the proliferation of HT29 colon cancer cells [19]. Similarly, cytotoxic effects in lung cancer cells mediated through ROS generation and mitochondrial apoptosis have been reported [20] .These findings collectively reinforce the potential of fengycin as a selective anticancer agent.

MicroRNAs (miRNAs) have recently emerged as promising therapeutic tools in cancer treatment. They regulate gene expression at the post-transcriptional level and play key roles in tumor progression and suppression [21,22].

Among them, miR-34a and MiR-34a are tumor suppressor miRNAs that inhibit cell proliferation and regulate apoptosis-related pathways [23,24]. These miRNAs function through the miRISC complex by binding to target mRNA and inhibiting its translation [25,26].

Importantly, the combination of fengycin with miR-34a significantly enhanced apoptosis in cancer cells. The apoptotic rate reached 71.6%, with increased TP53 and caspase-3 activity. In contrast, normal HGF cells showed low apoptosis (9.6%) and activation of survival genes such as PIK3CA and KRAS.

Overall, the miRNA–protein complex (30 μg/mL fengycin/2.5 nM miRNA) induced strong apoptotic signaling in cancer cells while preserving normal cell viability.

5. CONCLUSION

The miR-34a–fengycin complex (30 μg/mL fengycin/2.5 nM miRNA) exhibits a dual mechanism of action, combining membrane disruption and gene regulation. This leads to suppression of oncogenes and activation of apoptotic pathways. These findings highlight its potential as a selective anticancer strategy.

Although the present study demonstrated promising selective anticancer activity of the miR-34a–fengycin biocomplex against HCT116 colorectal cancer cells, several limitations should be acknowledged. First, the molecular findings were primarily based on gene expression analysis without additional protein-level validation such as Western blotting or pathway inhibition assays. Therefore, further mechanistic investigations are necessary to confirm the involvement of apoptotic and signaling pathways at the protein level.

Second, additional physicochemical characterization of the miR-34a–fengycin biocomplex, including particle size distribution, zeta potential measurement, binding efficiency, and stability analysis, was not performed in the current study and should be addressed in future investigations to strengthen formulation reproducibility and mechanistic understanding.

Furthermore, the present work was limited to an in vitro experimental model using HCT116 cells. Consequently, further validation using 3D culture systems and in vivo animal models is required to evaluate the efficacy, biosafety, pharmacokinetic behavior, and translational potential of the proposed therapeutic strategy.

Despite these limitations, the findings provide preliminary evidence supporting the potential of the miR-34a–fengycin biocomplex as a selective anticancer approach and establish a basis for future preclinical investigations.

Conflict of interest: Authors declare no conflicts of interest.

REFERENCES

1. Fink H, Langselius O, Vignat J, Rumgay H, Rehm J, et al. Global and regional cancer burden attributable to modifiable risk factors to guide prevention. Nat Med. Published online February 3, 2026.
2. Hameed MA, Hamed OM. Detection of P53 suppressor gene mutation in women with breast cancer in Mosul city. AIP Conf Proc. 2023;2834(1):020007. doi:10.1063/5.0161448.
3. Yan S, Zhan F, He Y, et al. p53 in colorectal cancer: From a master player to a privileged therapy target. J Transl Med. 2025;23:684. doi:10.1186/s12967-025-06566-4
4. Al-Hazmi NE. Antibacterial and anticancer activities of rhizobacterial lipopeptides against carcinogenic bacteria. Antonie Van Leeuwenhoek. 2025;118:118. doi:10.1007/s10482-025-02131-7.
5. Sur S, Romo TD, Grossfield A. Selectivity and mechanism of fengycin, an antimicrobial lipopeptide, from molecular dynamics. J Phys Chem B. 2018;122(8):2219-2226. doi:10.1021/acs.jpcb.7b11889.
6. Zihalirwa Kulimushi P, Argüelles Arias A, Franzil L, Steels S, Ongena M. Stimulation of fengycin-type antifungal lipopeptides in Bacillus amyloliquefaciens in the presence of the maize fungal pathogen Rhizomucor variabilis. Front Microbiol. 2017;8:850. doi:10.3389/fmicb.2017.00850.
7. Rezaeian O, et al. MicroRNA: A new gate in cancer and human disease: A review. J Biol Sci. 2017;17:247-254.
8. Kilikevicius A, Meister G, Corey DR. Reexamining assumptions about miRNA-guided gene silencing. Nucleic Acids Res. 2022;50(2):617-634. doi:10.1093/nar/gkab1256.
9. Freshney RI. Culture of animal cells: A manual of basic technique and specialized applications. 7th ed. John Wiley & Sons; 2015.
10. Piccinini F, Tesei A, Arienti C, et al. Cell counting and viability assessment of 2D and 3D cell cultures: Expected reliability of the trypan blue assay. Biol Proced Online. 2017;19:8. doi:10.1186/s12575-017-0056-3
11. Al-S'adoon RNH, Al-Rawi AM. A novel in vitro evidence on anticancer effect of local isolate Enterococcus faecalis bacteriocin. Zenodo. 2023. doi:10.5281/zenodo.7704670.
12. Mukherjee PK. Bioassay-guided isolation and evaluation of herbal drugs. In: Mukherjee PK, ed. Quality control and evaluation of herbal drugs. Elsevier; 2019:515-537. doi:10.1016/B978-0-12-813374-3.00013-2.
13. Livak KJ, Schmittgen TD. Analysis of relative gene expression data using real-time quantitative PCR and the 2−ΔΔCT method. Methods. 2001;25(4):402-408. doi:10.1006/meth.2001.1262.
14. Specchia M, Siringo M, Mazzotti E, Mazzuca F. Relationship between single-nucleotide polymorphisms and cancer immunotherapy efficacy and toxicity: A systematic review. Front Oncol. 2025;15:1653990. doi:10.3389/fonc.2025.1653990.
15. Yu X, Zhao H, Wang R, et al. Cancer epigenetics: From laboratory studies and clinical trials to precision medicine. Cell Death Discov. 2024;10:28. doi:10.1038/s41420-024-01803-z.
16. Dan AK, Manna A, Ghosh S, Sikdar S, Sahu R, Parhi PK, Parida S. Molecular mechanisms of the lipopeptides from Bacillus subtilis in the apoptosis of cancer cells: A review on its current status in different cancer cell lines. Adv Cancer Biol Metastasis. 2021;3:100019. doi:10.1016/j.adcanc.2021.100019.
17. Liu ZY, Yu XZ. Engineering Bacillus subtilis for high-value bioproduction: Recent advances and applications. Microb Cell Fact. 2025;24:182. doi:10.1186/s12934-025-02818-6.
18. Medeot DB, Fernandez M, Morales GM, Jofré E. Fengycin from Bacillus amyloliquefaciens MEP218 exhibit antibacterial activity by producing alterations on the cell surface of the pathogens Xanthomonas axonopodis pv. vesicatoria and Pseudomonas aeruginosa PAO1. Front Microbiol. 2020;10:3107. doi:10.3389/fmicb.2019.03107.
19. Cheng W, Feng Y, Ren J, Jing D, Wang C. Anti-tumor role of Bacillus subtilis fmbJ-derived fengycin on human colon cancer HT29 cell line. Neoplasma. 2016;63(2):215-222.
20. Yin H, Guo C, Wang Y, Liu D, Lv Y, Lv F, Lu Z. Fengycin inhibits the growth of the human lung cancer cell line 95D through reactive oxygen species production and mitochondria-dependent apoptosis. Anticancer Drugs. 2023;24(6):587-598. doi:10.1097/CAD.0b013e3283611395.
21. Zare E, Yaghoubi SM, Khoshnazar M, Jafari Dargahlou S, Machhar JS, Zheng Z, Duijf PHG, Mansoori B. MicroRNAs in cancer immunology: Master regulators of the tumor microenvironment and immune evasion, with therapeutic potential. Cancers (Basel). 2025;17(13):2172. doi:10.3390/cancers17132172
22. Shi Y, Zheng H, Wang T, et al. Targeting KRAS: From metabolic regulation to cancer treatment. Mol Cancer. 2025;24:9. doi:10.1186/s12943-024-02216-3.

23. Soliman B, Ibrahim AF, Salem A, Ghazy M, Abo-Elfadl MT, ElHefnawi M, Flores M. Let-7a and miR-34a interplay potent suppressive roles in hepatocellular carcinoma via co-targeting FNDC3B, IGF2 and SOX4. Int J Mol Sci. 2026;27(4):1714. doi:10.3390/ijms27041714
24. Zhang L, Liao Y, Tang L. MicroRNA-34 family: A potential tumor suppressor and therapeutic candidate in cancer. J Exp Clin Cancer Res. 2019;38:53. doi:10.1186/s13046-019-1059-5
25. Chatterjee T, Mandal S, Ray S, Johnson-Buck A, Walter NG. A unifying model for microRNA-guided silencing of messenger RNAs. Nat Commun. 2025. doi:10.1038/s41467-025-67186-6
26. Fu P, Guo Y, Luo Y, Mak M, Zhang J, Xu W, Qian H, Tao Z. Visualization of microRNA therapy in cancers delivered by small extracellular vesicles. J Nanobiotechnol. 2023;21(1):457. doi:10.1186/s12951-023-02187-5.
27. Yaser Jasem Mohammed Alkhatony, Ph.D. in Microbiology, Laboratory of Microbiology, Al-Baaj General Hospital, Nineveh Health Directorate, Ministry of Health, Mosul, Iraq.
28. E-mail: Yaser.23scp153@student.uomosul.edu.iq. ORCID: 0000-0001-5561-5406
29. Mahmood Abduljabar Altobje, Ph.D. in Microbiology, Department of Biology, College of Science, University of Mosul, Mosul, Iraq. E-mail: mahtsbio30@uomosul.edu.iq. ORCID: 0009-0007-1402-0749
30. Mahmood Ahmad Aboo, MD, Specialist in Internal Medicine, Al-Baaj General Hospital, Nineveh Health Directorate, Ministry of Health, Mosul, Iraq. E-mail: rp332vh7@gmail.com. ORCID: 0009-0007-1405-0489